Mechanics Research Communications 38 (2011) 214–219

Contents lists available at ScienceDirect

Mechanics Research Communications

journal homepage: www.elsevier.com/locate/mechrescom

Dynamic near three-to-one internal resonance in composite stiffened panels

Abdellah Karimin, Mohamed Belhaq*

Laboratory of Mechanics, University Hassan II, Casablanca, Morocco

ARTICLE INFO

Article history:
Received 28 October 2009
Received in revised form
29 November 2010
Available online 5 March 2011

Keywords:
Internal resonance
Stiffened panels
Composite materials
Modal interaction

ABSTRACT

Nonlinear dynamic of composite stiffened panels to parametric and three-to-one internal resonances is investigated. The ordinary differential equation of two mode shapes is established by using Galerkin method and the condition of three-to-one internal resonance between the first mode (1,3) and the second mode (3,1) is examined near the principal resonance 2:1 of the first mode. Then, the nonlinear behavior of the two buckling mode shapes is analyzed using a perturbation analysis. We show the existence of jump phenomena for the two modes indicating a complex dynamic of the structure near the three-to-one internal resonance for the HM Graphite/epoxy materials.

1. Introduction

Stiffened composite laminated panels are widely used in many engineering applications. Depending on its geometry and stiffness, a stiffened plate can exhibit different buckling modes. Elishakoff et al. (1995) investigated the effect of small structural irregularity on the buckling load and the buckling mode of a rib-stiffened plate. Shin (1999) examined the post-buckling behavior of rectangular isotropic stiffened plates under in-plane compressive load. Sapountzakis and Mokos (2008) established a general solution for the analysis of plates stiffened by arbitrary placed parallel beams of arbitrary doubly symmetric cross with deformable connection subjected to an arbitrary loading. Karimin and Belhaq (2009) examined the effect of stiffener on nonlinear characteristic behavior of a rectangular plate using a single mode approach. For other applications, see Chien and Chen (2005), Featherston and Watson (2006), Amabili and Farhadi (2009), Prusty (2008) and Bisagni and Vescovini (2009). For a brief review of nonlinear modal interaction, we refer the reader, for instance, to Chin and Nayfeh (1999) and Touzé et al. (2002).

In this work, we perform an analytical treatment to investigate nonlinear modal interaction of a composite stiffened panel subjected to axial compression. We consider a plate composed of finite number of orthotropic layers. The differential equation of the deflection surface is established using Von Karman approximation and classical lamination theory. The ordinary differential equations of the two mode shapes are established using Galerkin's method. Then, the condition of three-to-one internal resonance between the first mode (1,3) and the second mode (3,1) is examined using the multiple scale technique (Nayfeh and Mook, 1979).

2. Problem formulation

2.1. Local equations

The problem formulation of composite longitudinally stiffened panels is organized as shown in Fig. 1a. We study the complete structure using the portion of panel between stiffeners, as shows in Fig. 1b by considering a plate of constant thickness h composed of a finite number of orthotropic layers. Assume that the middle plane of the plate coincides with the x-y plane, and the z-axis is normal to the middle plane. The Von Karman nonlinear strains are given by

$$\varepsilon_{11} = e_1 - zw_{xx}, \varepsilon_{22} = e_2 - zw_{yy}, \varepsilon_{12} = \gamma_6 - 2zw_{xy},$$
$$\varepsilon_{33} = \varepsilon_{13} = \varepsilon_{23} = 0 \quad (1)$$

$$e_1 = u_x + \frac{1}{2}w_x^2, e_2 = v_y + \frac{1}{2}w_y^2, \gamma_6 = u_y + v_x + w_x w_y \quad (2)$$

here u, v, w are displacement components along x, y, z directions, respectively. The governing equations of the problem obtained by applied the Hamilton principle can be stated as

$$\int_0^t (\delta T - \delta \Pi + \delta W_{nc})dt = 0 \quad (3)$$

where δW_{nc} denotes variation of the nonconservative energy W_{nc}, while variations of the kinetic and elastic energies T and Π are

* Corresponding author.
E-mail address: mbelhaq@yahoo.fr (M. Belhaq).

0093-6413/$ – see front matter © 2011 Elsevier Ltd. All rights reserved.
doi:10.1016/j.mechrescom.2011.02.003

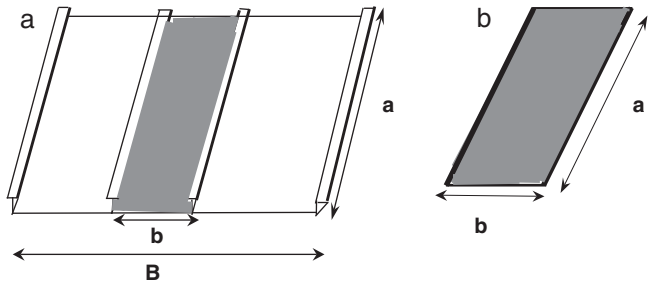

Fig. 1. (a) Complete stiffened and structure modelled portion. (b) Portion of panels elastically restrained along unload edges.

given, respectively, by

$$\delta T = -\int_z \int_A \rho \ddot{D}.\delta D dA dz \tag{4}$$

$$\delta \Pi = \int_z \int_A (\sigma_{11}\delta\varepsilon_{11} + \sigma_{22}\delta\varepsilon_{22} + \sigma_{33}\delta\varepsilon_{33} + \sigma_{23}\delta\varepsilon_{23} + \sigma_{13}\delta\varepsilon_{13} + \sigma_{12}\delta\varepsilon_{12}) dA dz \tag{5}$$

where ρ is the mass density, A denotes the undeformed area of the reference plane, D is the displacement vector of an arbitrary point of the differential plate element under observation, the σ_{ij} are the Jaumann stresses, and the ε_{ij} are the Jaumann strains (Nayfeh and Pai, 2004).

Substituting Eqs. (1) and (2) into Eq. (5) yields

$$\delta \Pi = \int_z \int_A [\sigma_{11}(\delta u_x + w_x \delta w_x - z\delta w_{xx}) + \sigma_{22}(\delta v_y + w_y \delta w_y - z\delta w_{yy}) + \sigma_{12}(\delta u_y + \delta v_x + w_x \delta w_y + w_y \delta w_x - 2z\delta w_{xy})] dA dz \tag{6}$$

Neglecting in-plane inertia terms, the equations of equilibrium read

$$N_{1,x} + N_{6,y} = 0,\ N_{6,x} + N_{2,y} = 0,\ M_{1,xx} + 2M_{6,xy} + M_{2,yy} + (N_1 w_x + N_6 w_y)_x + (N_6 w_x + N_2 w_y)_y = \rho h \ddot{w} + \mu h \dot{w} \tag{7}$$

The internal forces N_i and M_i are related to the midplane strains and curvatures as

$$\begin{bmatrix} N_1 \\ N_2 \\ N_6 \\ M_1 \\ M_2 \\ M_6 \end{bmatrix} = \begin{bmatrix} A_{ij} & B_{ij} \\ B_{ij} & D_{ij} \end{bmatrix} \begin{bmatrix} e_1 \\ e_2 \\ \gamma_6 \\ -w_{xx} \\ -w_{yy} \\ -2w_{xy} \end{bmatrix} \tag{8}$$

For a symmetric cross-play laminate, we have

$$[B_{ij}] = 0, \quad [A_{ij}] = \begin{bmatrix} A_{11} & A_{12} & 0 \\ A_{12} & A_{22} & 0 \\ 0 & 0 & A_{66} \end{bmatrix}, \quad [D_{ij}] = \begin{bmatrix} D_{11} & D_{12} & 0 \\ D_{12} & D_{22} & 0 \\ 0 & 0 & D_{66} \end{bmatrix} \tag{9}$$

and for a plate made of a single orthotropic material, one obtains

$$[A_{ij}] = \frac{h}{(1-\nu_{12}\nu_{21})} \begin{bmatrix} E_{11} & \nu_{21}E_{11} & 0 \\ \nu_{21}E_{11} & E_{22} & 0 \\ 0 & 0 & G_{12}(1-\nu_{12}\nu_{21}) \end{bmatrix}, \quad [D_{ij}] = \frac{1}{12}h^2[A_{ij}] \tag{10}$$

Eq. (7) can be satisfied exactly by introducing the stress function $F(x, y, t)$ defined by

$$N_1 = F_{yy}, \quad N_2 = F_{xx}, \quad N_6 = -F_{xy} \tag{11}$$

Then, Eq. (7) becomes

$$M_{1,xx} + 2M_{6,xy} + M_{2,yy} + w_{xx}F_{yy} - 2w_{xy}F_{xy} + w_{yy}F_{xx} = \rho h \ddot{w} + ch\dot{w} \tag{12}$$

and the compatibility equation is written as

$$e_{1,yy} + e_{1,xx} - 2e_{6,xy} = (w_{xy})^2 - w_{xx}w_{yy} \tag{13}$$

in which

$$e_1 = S_{11}F_{yy} + S_{12}F_{xx},\ e_2 = S_{12}F_{yy} + S_{22}F_{xx},\ 2e_6 = -S_{66}F_{xy} \tag{14}$$

where $(S_{11}, S_{12}, S_{22}) = ((A_{22}, -A_{12}, A_{11})/A_{11}A_{22} - A_{12}^2)$ and $s_{66} = 1/A_{66}$. Substituting Eq. (14) into Eq. (13), we obtain the second equation:

$$S_{22}F_{xxxx} + (2S_{12} + S_{66})F_{xxyy} + S_{11}F_{yyyy} = (w_{xy})^2 - w_{xx}w_{yy} \tag{15}$$

The moment and the transverse displacement $w(x, y, t)$ are related by

$$\begin{bmatrix} M_1 \\ M_2 \\ M_6 \end{bmatrix} = -\begin{bmatrix} D_{11} & D_{12} & 0 \\ D_{12} & D_{22} & 0 \\ 0 & 0 & D_{66} \end{bmatrix} \begin{bmatrix} w_{xx} \\ w_{yy} \\ w_{xy} \end{bmatrix} \tag{16}$$

Then, Eq. (12) can be rewritten as

$$\rho h \ddot{w} + \mu h \dot{w} + D_{11}w_{xxxx} + 2(D_{12} + 2D_{66})w_{xxyy} + D_{22}w_{yyyy} = w_{xx}F_{yy} - 2w_{xy}F_{xy} + w_{yy}F_{xx} \tag{17}$$

The in-plane excitation of the laminated panels $P = P_0 - P_d\cos(\Omega t)$ is applied to the edges perpendicular to the direction of the stiffeners, and the loaded edges are considered simply supported. The boundary conditions are written as

$$v = w = M_x = 0 \ \text{ and } \ \int_0^b \frac{\partial^2 F}{\partial y^2} dy = -bhP \ \text{ at } \ x = 0,\ a \tag{18}$$

$$w = 0 \ \text{ and } \ M_y = -(D_{12}w_{xx} + D_{22}w_{yy}) = GJ\frac{\partial^3 w}{\partial x^2 \partial y} \text{ at } \ y = 0, b \tag{19}$$

where GJ is the torsional rigidity of the stiffeners.

Introducing the following variables and parameter transformations

$$\bar{w} = \frac{w}{h}, \bar{x} = \frac{x}{a}, \bar{y} = \frac{y}{b}, \bar{F} = \frac{F}{D^*}, \lambda = \frac{a}{b}, \bar{\mu} = a^2\frac{1}{\sqrt{\rho h D^*}}\mu,$$

$$\bar{P} = \frac{b^2 h}{D^*}P, \tau = \frac{1}{a^2}\sqrt{\frac{D^*}{\rho h}}t, \lambda = \frac{a}{b}, D^* = \frac{E_{22}h^3}{12(1-\nu_{12}\nu_{21})} \tag{20}$$

Eqs. (15), (17), (18) and (19) can be rewritten in nondimensional form as

$$\ddot{\bar{w}} + \bar{\mu}\dot{\bar{w}} + \delta\bar{w}_{xxxx} + 2\lambda^2\left(\nu_{12} + \frac{2}{f}\left(1 - \frac{\nu_{12}^2}{\delta}\right)\right)\bar{w}_{xxyy} + \lambda^4\bar{w}_{yyyy} = \lambda^2[\bar{w}_{xx}\bar{F}_{yy} - 2\bar{w}_{xy}\bar{F}_{xy} + \bar{w}_{yy}\bar{F}_{xx}] \tag{21}$$

$$\delta F_{xxxx} + (f - 2\nu_{12})F_{xxyy} + \lambda^4 F_{yyyy} = 12\lambda^2\left(1 - \frac{\nu_{12}^2}{\delta}\right)[(w_{xy})^2 - w_{xx}w_{yy}] \tag{22}$$

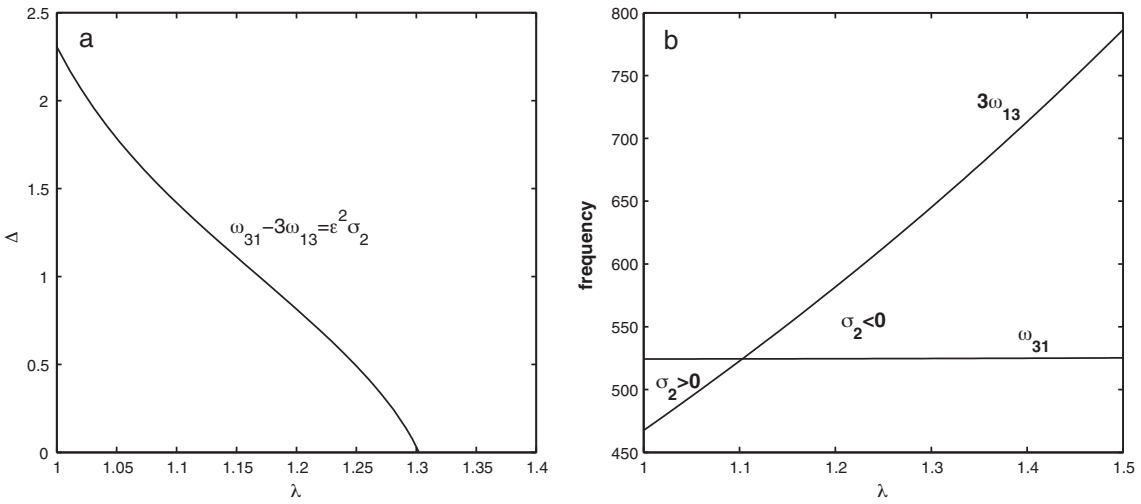

Fig. 2. Internal resonance. (a) Torsional rigidity of the stiffeners versus λ. (b) Variation of three times the ω_{13} natural frequency and the ω_{13} versus λ for $\Delta = 1.4$.

$$v = w = M_x = \left(\bar{w}_{xx} + \frac{\nu_{12}\lambda^2}{\delta}\bar{w}_{yy}\right) = 0 \text{ and } \int_0^1 \frac{\partial^2 \bar{F}}{\partial y^2} dy = -\bar{P} \text{ at } x = 0, 1 \tag{23}$$

$$\bar{w} = 0 \text{ and } M_y = -(\nu_{12}\bar{w}_{xx} + \lambda^2\bar{w}_{yy}) = \Delta\frac{\partial^3 \bar{w}}{\partial x^2 \partial y} \text{ at } y = 0, 1 \tag{24}$$

where $\Delta = (GJ/bD)$, $\delta = (E_{11}/E_{22})$ and $f = (E_{22}/G_{12})$. Using the Galerkin technique, the deflection surface is taken as in (Shin, 1999; Bisagni and Vescovini, 2009) and given by

$$w(x, y) = \sum_{m=1,3}^{\infty}\sum_{n=1,3}^{\infty} \sin(m\pi x)[W_{mn}\sin(n\pi y) + \bar{W}_{mn}(1 - \cos(2n\pi y))] \tag{25}$$

where the terms W_{nn}, $\bar{W}_{mn}$ represent the amplitudes of functions that satisfy simply supported and clamped conditions, respectively. The equilibrium conditions between plate bending moments and stiffener torsional moments are given by Eq. (24). Substituting Eq. (25) into Eq. (24), the assumed form of out-of-plane displacement reads

$$w(x, y) = \sum_{m=1,3}^{\infty}\sum_{n=1,3}^{\infty} W_{mn}\ \sin(m\pi x)[\sin(n\pi y) + \gamma_{mn}(1 - \cos(2n\pi y))] \tag{26}$$

where $\gamma_{mn} = (m^2\pi/4n\lambda^2)\Delta$. We focus attention on the nonlinear oscillations of a laminated stiffened panel in the first two modes (1,3) and (3,1). Thus, we write the w in the form:

$$w(x, y, t) = q_1(t)\psi_1(x, y) + q_2(t)\psi_2(x, y) \tag{27}$$

where $\psi_1(x, y) = \sin(\pi x)[\sin(3\pi y) + \gamma_{13}(1 - \cos(6\pi y))]$ and $\psi_2(x, y) = \sin(3\pi x)[\sin(\pi y) + \gamma_{31}(1 - \cos(2\pi y))]$. Substituting Eq. (27) into Eq. (22), considering the boundary conditions, Eq. (23), and integrating, we obtain the stress function as follows:

$$\begin{aligned}\bar{F}(x, y, t) = &-\frac{1}{2}\bar{P}y^2 + c_1(t)\cos(2\pi x) + c_2(t)\cos(6\pi x) + c_3(t)\cos(2\pi y)\\ &+ c_4(t)\cos(4\pi y) + c_5(t)\cos(6\pi y)\\ &+ c_6(t)\cos(12\pi y) + c_7(t)\sin(\pi y)\\ &+ c_8(t)\sin(3\pi y) + c_9(t)\sin(9\pi y)\\ &+ \sum_{10}^{17} c_k(t)\cos(i\pi x)\cos(j\pi y) + \sum_{18}^{28} c_k(t)\cos(p\pi x)\sin(q\pi y)\end{aligned} \tag{28}$$

where $(i, j) = \{(2,2), (2,4), (2,6), (2,8), (4,2), (4,4), (4,8), (6,2)\}$.$(p, q) = \{(2,1), (2,3), (2,5), (2,7), (2,9), (4,1), (4,3), (4,5), (4,7), (6,1), (6,3)\}$.Substituting Eqs. (27) and (28) into Eq. (21), dropping the bars and integrating, we obtain the following dimensionless equations of motion:

$$\begin{aligned}&\ddot{q}_1(t) + \mu\dot{q}_1(t) + (\omega_{13}^2 + \Gamma_1 P_d\cos(\Omega t))q_1(t) + \Gamma_2 q_2(t)^2 q_1(t)\\ &+ \Gamma_3 q_2(t)q_1(t)^2 + \Gamma_4 q_1(t)^3 = 0\end{aligned} \tag{29}$$

$$\begin{aligned}&\ddot{q}_2(t) + \mu\dot{q}_2(t) + (\omega_{31}^2 + \xi_1 P_d\cos(\Omega t))q_2(t) + \xi_2 q_1(t)^3\\ &+ \xi_3 q_1(t)^2 q_2(t) + \xi_4 q_2(t)^3 = 0\end{aligned} \tag{30}$$

here, we examine the occurrence condition of internal resonance between the (1,3) mode and the (3,1) mode for the HM Graphite/epoxy materials by plotting the equation $\omega_{31}(\Delta, \lambda) - 3\omega_{13}(\Delta, \lambda) = 0$. The material properties for HM Graphite/epoxy are given as: $\nu_{12} = 0.25$, $\delta = 34.848$ and $f = 1.375$. Fig. 2a shows that a three-to-one internal resonance ($\omega_{31} \simeq 3\omega_{13}$) is possible for a certain range of the parameter plane (λ, Δ). Fig. 2b shows the variation of the frequency ω_{13} and the frequency ω_{31}.

3. Method of analysis

To analyze the periodic response of the system (29) and (30) for weak damping and nonlinearity, we use the method of multiple scales by seeking a second-order uniform expansion in the form:

$$\begin{aligned}q_1(t) &= \varepsilon q_{11}(T_0, T_2) + \varepsilon^3 q_{13}(T_0, T_2)\\ q_2(t) &= \varepsilon q_{21}(T_0, T_2) + \varepsilon^3 q_{23}(T_0, T_2)\end{aligned} \tag{31}$$

where $T_0 = t$ is the slow scale characterizing motions at the natural frequencies and $T_2 = \varepsilon^2 t$ is a fast scale characterizing the modulation of the amplitude and phase. We scale the damping μ and the forcing as $\mu = \varepsilon^2\tilde{\mu}$ and $P_d = \varepsilon^2\tilde{P}_d$. Substituting Eq. (31) into (29) and (30) and equating coefficients of like powers of ε, we obtain at different orders

$$D_0^2 q_{11} + \omega_{13}^2 q_{11} = 0,\ D_0^2 q_{21} + \omega_{31}^2 q_{21} = 0 \tag{32}$$

and

$$\begin{aligned}D_0^2 q_{13} + \omega_{13}^2 q_{13} = &-[2D_0 D_2 q_{11} + \tilde{\mu}D_0 q_{11} + \Gamma_1\tilde{P}_d\cos(\Omega T_0)q_{11}\\ &+ \Gamma_2 q_{21}^2 q_{11} + \Gamma_3 q_{21} q_{11}^2 + \Gamma_4 q_{11}^3]\end{aligned} \tag{33}$$

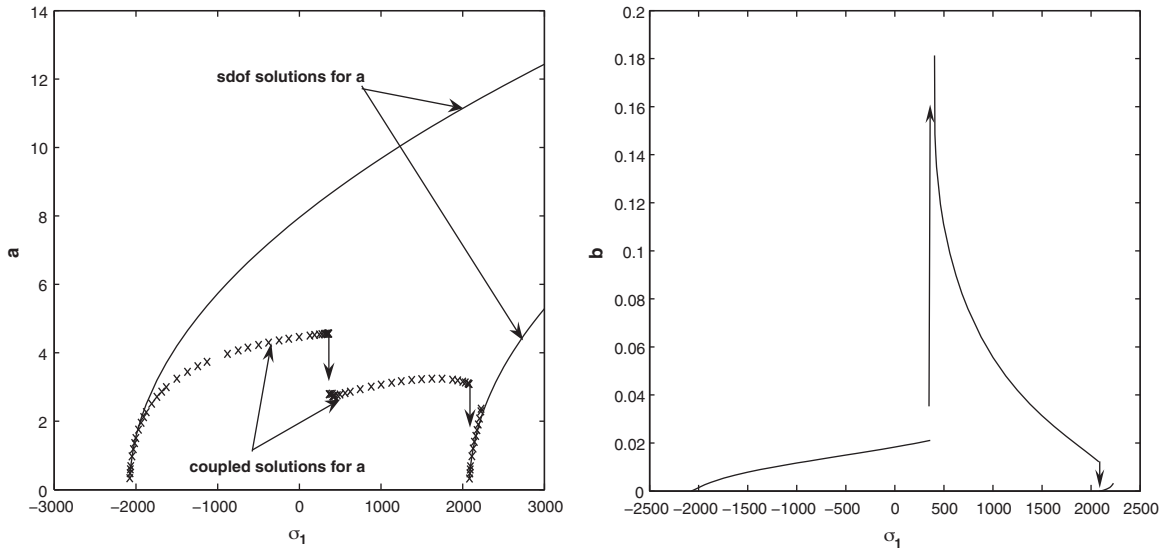

Fig. 3. Frequency response curves for the two modes: λ=1.25, ε = 0.1 and Δ = 0.5028.

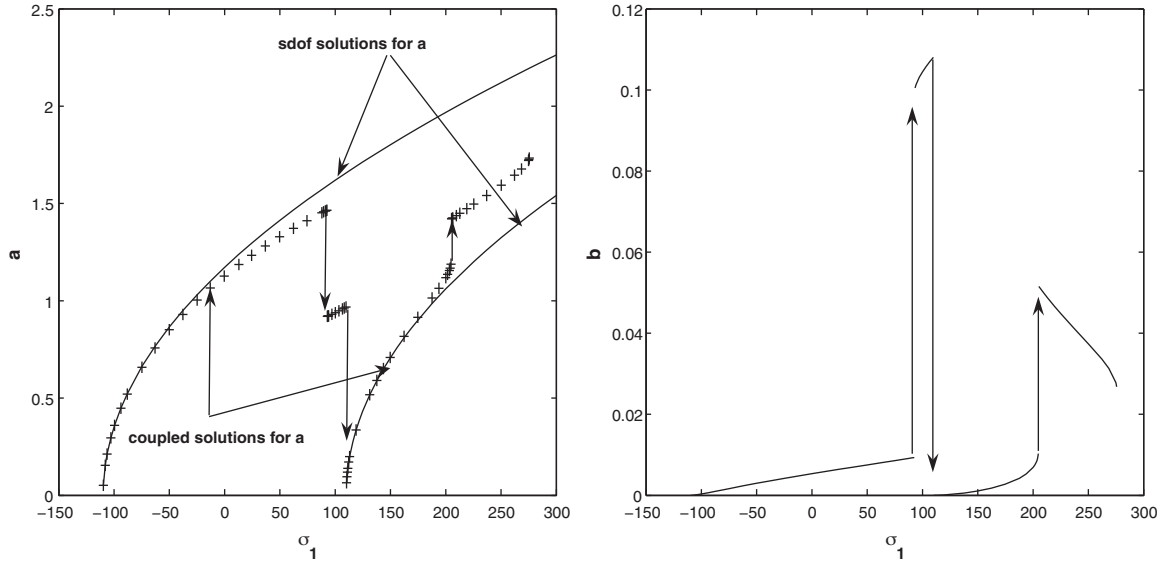

Fig. 4. Frequency response curves for the two modes: λ = 1.15, ε = 0.1 and Δ = 1.121.

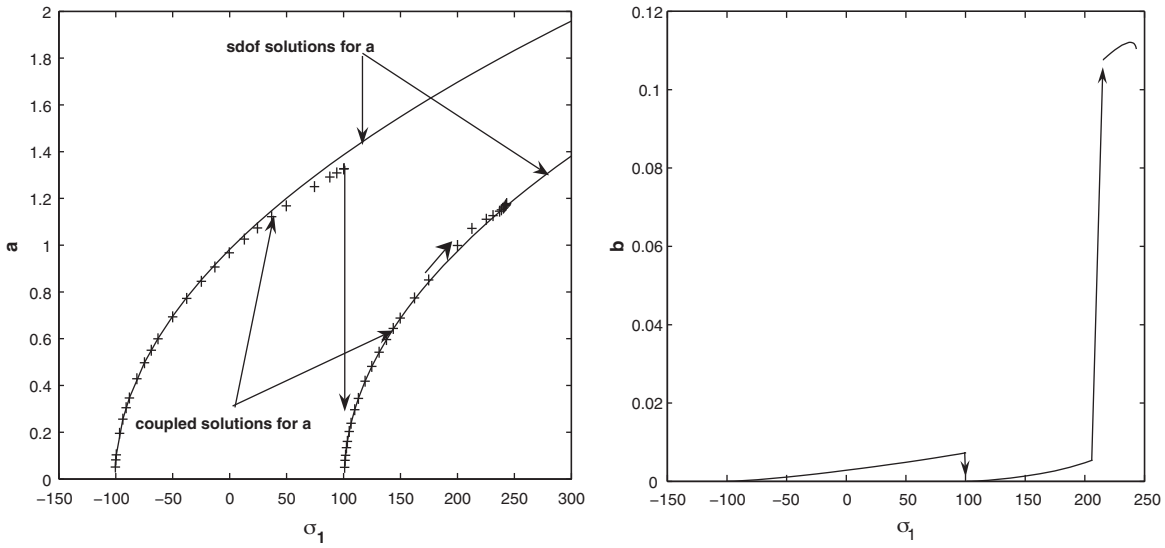

Fig. 5. Frequency response curves for the two modes: λ = 1.1, ε = 0.1 and Δ = 1.419.

$$D_0^2 q_{23} + \omega_{31}^2 q_{23} = -[2D_0 D_2 q_{21} + \tilde{\mu} D_0 q_{21} + \xi_1 \tilde{P}_d \cos(\Omega T_0) q_{21} + \xi_2 q_{11}^3 + \xi_3 q_{11}^2 q_{21} + \xi_4 q_{21}^3] \quad (34)$$

where $D_k = \partial/\partial T_k$. To proceed further, we describe the nearness of ω_{31} to $3\omega_{13}$ and Ω to $2\omega_{13}$ by introducing the detuning parameters σ_1 and σ_2 as

$$\omega_{31} = 3\omega_{13} + \varepsilon^2 \sigma_2, \quad \Omega = 2\omega_{13} + \varepsilon^2 \sigma_1 \quad (35)$$

The solution of Eq. (32) can be expressed as

$$q_{11}(T_0, T_2) = A(T_2) e^{i\omega_{13} T_0} + cc,\ q_{21}(T_0, T_2) = B(T_2) e^{i\omega_{31} T_0} + cc \quad (36)$$

where cc denotes the complex conjugate of the preceding terms. The quantities $A(T_2)$ and $B(T_2)$ are determined by eliminating the secular terms at the next level of approximations. Substituting Eqs. (36) into Eqs. (33) and (34) and eliminating secular terms give

$$D_2 A = -\frac{\tilde{\mu}}{2} A + i \frac{\Gamma_1 \tilde{P}_d}{4\omega_{13}} \bar{A} e^{i\sigma_1 T_2} + i \frac{\Gamma_2}{\omega_{13}} A|B|^2 + i \frac{\Gamma_3}{2\omega_{13}} \bar{A}^2 B e^{i\sigma_2 T_2} + i \frac{3\Gamma_4}{2\omega_{13}} \bar{A}|A|^2 \quad (37)$$

$$D_2 B = -\frac{\tilde{\mu}}{2} B + i \frac{\xi_2}{2\omega_{31}} A^3 e^{-i\sigma_2 T_2} + i \frac{\xi_3}{\omega_{31}} |A|^2 B + i \frac{3\xi_4}{2\omega_{31}} \bar{B}|B|^2 \quad (38)$$

Letting $A = a(T_2) e^{i\theta(T_2)}$ and $B = b(T_2) e^{i\phi(T_2)}$ where a, b, θ and ϕ are real functions, separating real and imaginary parts, we obtain the slow flow modulation equations of amplitudes and phases. This system can be transformed into an autonomous one when defining

$$\gamma_1 = \frac{1}{2}\sigma_1 T_2 - \theta, \quad \gamma_2 = \left(\frac{3}{2}\sigma_1 - \sigma_2\right) T_2 - \phi \quad (39)$$

One finally obtains

$$\frac{da}{dt} = -\frac{\mu}{2} a - \frac{\Gamma_1 P_d}{4\omega_{13}} a \sin(2\gamma_1) + \frac{\varepsilon^2 \Gamma_3}{2\omega_{13}} a^2 b \sin(\gamma_2 - 3\gamma_1) \quad (40)$$

$$a \frac{d\gamma_1}{dt} = \frac{\varepsilon^2 \sigma_1}{2} a - \frac{\Gamma_1 P_d}{4\omega_{13}} a \cos(2\gamma_1) - \frac{\varepsilon^2 \Gamma_2}{\omega_{13}} a b^2 - \frac{\varepsilon^2 \Gamma_3}{2\omega_{13}} a^2 b \cos(\gamma_2 - 3\gamma_1) - \frac{3\varepsilon^2 \Gamma_4}{2\omega_{13}} a^3 \quad (41)$$

$$\frac{db}{dt} = -\frac{\mu}{2} b - \frac{\varepsilon^2 \xi_2}{2\omega_{31}} a^3 \sin(\gamma_2 - 3\gamma_1) \quad (42)$$

$$b \frac{d\gamma_2}{dt} = \varepsilon^2 \left(\frac{3}{2}\sigma_1 - \sigma_2\right) b - \frac{\varepsilon^2 \xi_2}{2\omega_{31}} a^3 \cos(\gamma_2 - 3\gamma_1) - \frac{\varepsilon^2 \xi_3}{\omega_{31}} a^2 b - \frac{3\varepsilon^2 \xi_4}{2\omega_{31}} b^3 \quad (43)$$

Equilibria of the slow flow (40)–(43) correspond to periodic solutions of Eqs. (29) and (30). These are obtained by setting, in system (40)–(43), $(da/dt) = (d\gamma_1/dt) = (db/dt) = (d\gamma_2/dt) = 0$. We obtain

$$-\frac{\mu}{2} a + \frac{\varepsilon^2 \Gamma_3}{2\omega_{13}} a^2 b \sin(\gamma_2 - 3\gamma_1) = \frac{\Gamma_1 P_d}{4\omega_{13}} a \sin(2\gamma_1) \quad (44)$$

$$\frac{\varepsilon^2 \sigma_1}{2} a - \frac{\varepsilon^2 \Gamma_2}{\omega_{13}} a b^2 - \frac{3\varepsilon^2 \Gamma_4}{2\omega_{13}} a^3 - \frac{\varepsilon^2 \Gamma_3}{2\omega_{13}} a^2 b \cos(\gamma_2 - 3\gamma_1) = \frac{\Gamma_1 P_d}{4\omega_{13}} a \cos(2\gamma_1) \quad (45)$$

$$-\frac{\mu}{2} b = \frac{\varepsilon^2 \xi_2}{2\omega_{31}} a^3 \sin(\gamma_2 - 3\gamma_1) \quad (46)$$

$$\varepsilon^2 \left(\frac{3}{2}\sigma_1 - \sigma_2\right) b - \frac{\varepsilon^2 \xi_3}{\omega_{31}} a^2 b - \frac{3\varepsilon^2 \xi_4}{2\omega_{31}} b^3 = \frac{\varepsilon^2 \xi_2}{2\omega_{31}} a^3 \cos(\gamma_2 - 3\gamma_1) \quad (47)$$

4. Solutions and bifurcation

In this section, we analyze the frequency response curves using the system (44)–(47). Indeed, Eqs. (46) and (47) can give the following expressions:

$$\sin(\gamma_2 - 3\gamma_1) = -\frac{\mu \omega_{31}}{\varepsilon^2 \xi_2 a^3} b, \quad \cos(\gamma_2 - 3\gamma_1) = \frac{2\omega_{31}}{\xi_2 a^3} \left[\left(\frac{3}{2}\sigma_1 - \sigma_2\right) b - \frac{\xi_3}{\omega_{31}} a^2 b - \frac{3\xi_4}{2\omega_{31}} b^3\right] \quad (48)$$

Eliminating the angles in system (44)–(47) gives the general relations for equilibria

$$\left(\frac{\Gamma_1 P_d}{4\omega_{13}} a\right)^2 = \left[\frac{\mu}{2}\left(a + \frac{\Gamma_3 \omega_{31} b^2}{\xi_2 \omega_{13} a}\right)\right]^2 + \left[\frac{\varepsilon^2 \sigma_1}{2} a - \frac{\varepsilon^2 \Gamma_2}{\omega_{13}} a b^2 - \frac{3\varepsilon^2 \Gamma_4}{2\omega_{13}} a^3 - \frac{\varepsilon^2 \Gamma_3}{\omega_{13}} \frac{\omega_{31}}{\xi_2} a b \left(\left(\frac{3}{2}\sigma_1 - \sigma_2\right) b - \frac{\xi_3}{\omega_{31}} a^2 b - \frac{3\xi_4}{2\omega_{31}} b^3\right)\right]^2 \quad (49)$$

$$\left(\frac{\mu \omega_{31}}{\varepsilon^2 \xi_2 a^3} b\right)^2 + \left[\frac{2\omega_{31}}{\xi_2 a^3}\left(\left(\frac{3}{2}\sigma_1 - \sigma_2\right) b - \frac{\xi_3}{\omega_{31}} a^2 b - \frac{3\xi_4}{2\omega_{31}} b^3\right)\right]^2 = 1 \quad (50)$$

Figs. 3–5 given by Eqs. (49) and (50) illustrate the frequency response of the two modes for different values of detuning $\varepsilon^2\sigma_2$ and for $P_0 = 5\pi^2$, $P_d = 3\pi^2$ and $\mu = 0.1$. Note that the coupled solution for the a-mode is designated by crosses, while the coupled solution for the b-mode is designated by solid lines in the b-mode figures. Fig. 3 corresponds to $\varepsilon^2\sigma_2 = -1.004$, Fig. 4 corresponds to $\varepsilon^2\sigma_2 = -0.93$, while Fig. 5 is plotted for $\varepsilon^2\sigma_2 = 0.0466$. The plots given in these figures indicate that for values of $\varepsilon^2\sigma_2$ smaller than -1, the stable periodic solution undergoes two bifurcations resulting in jump phenomena. In the first bifurcation the amplitude of the a-mode jumps down whereas the amplitude of the b-mode jumps up (see Fig. 3). In the second bifurcation, the amplitude of the two modes jumps down simultaneously.

For values of $\varepsilon^2\sigma_2$ lying between -1 and 0, the stable periodic solutions undergo three bifurcations (see Fig. 4). In the first bifurcation the amplitudes of the two modes behave as in the previous situation (a-mode jumps down, while b-mode jumps up). In the two other bifurcations, the amplitude of the two modes jumps in the same direction simultaneously.

For values of $\varepsilon^2\sigma_2$ greater than 0, the stable periodic solutions undergo two bifurcations and the amplitude of the two mode jumps simultaneously in the same direction (see Fig. 5). Figs. 3 and 4 show that the a-mode has a hardening characteristic, while the b-mode may have a softening or hardening characteristic (see the b-mode in Figs. 3 and 4).

5. Conclusion

In this work, we have investigated analytically nonlinear modal interaction of a composite stiffened panel subjected to axial compression. We have analyzed the nonlinear behavior of the two buckling mode shapes near the principal resonance 2:1 of the first mode (1,3) and three-to-one internal resonance $\omega_{31} \simeq 3\omega_{13}$ using

a perturbation analysis. The results shown that the two mode solutions coexist and the first mode clearly dominates the second mode. Further, the results indicate that the two modes can undergo several jumps when varying the detuning parameter σ_1. The jumps in the amplitudes may occur simultaneously in the same direction or in the opposite direction depending on the bifurcation location. Also, it was seen that the characteristic behavior of the second mode (3,1) can be of hardening or of softening type, while the first mode (1,3) is always softening. The existence of jump phenomena indicates the complexity of the dynamic near the 2:1 parametric resonance and the 3:1 internal resonance for the HM Graphite/epoxy materials.

References

Amabili, M., Farhadi, S., 2009. Shear deformable versus classical theories for nonlinear vibrations of rectangular isotropic and laminated composite plates. Journal of Sound and Vibration 320, 649–667.

Bisagni, C., Vescovini, R., 2009. Analytical formulation for local buckling and post-buckling analysis of stiffened laminated panels. Thin-Walled Structures 47, 318–334.

Chin, C.M., Nayfeh, A.H., 1999. Three to one internal resonances in parametrically excited hing clamped beams. Nonlinear Dynamics 20, 131–158.

Chien, R., Chen, C., 2005. Nonlinear vibration of laminated plates on a nonlinear elastic foundation. Composite Structures 70, 90–99.

Elishakoff, I., Li, Y.W., Starnes, J.R.J.H., 1995. Buckling mode localization in elastic plates due to misplacement in the stiffener location. Chaos, Solitons and Fractals 5 (8), 1517–1531.

Featherston, C.A., Watson, A., 2006. Buckling of optimized curved composite panels under shear and in-plane bending. Composites Science and Technology 66, 2878–2894.

Karimin, A., Belhaq, M., 2009. Effect of stiffener on nonlinear characteristic behavior of a rectangular plate: a single mode approach. Mechanics Research Communications 36, 699–706.

Nayfeh, A.H., Mook, D.T., 1979. Nonlinear Oscillations. Wiley-Interscience, New York.

Nayfeh, A.H., Frank Pai, P., 2004. Linear and Nonlinear Structural Mechanics. Wiley-Interscience, New York.

Prusty, B.G., 2008. Free vibration and buckling response of hat-stiffened composite panels under general loading. International Journal of Mechanical Sciences 50, 1326–1333.

Shin, ku.D., 1999. Post-buckling behavior of rectangular stiffened plates considering buckled pattern change. KSCE Journal of Civil Engineering 3 (4), 319–330.

Sapountzakis, E.J., Mokos, V.G., 2008. An improved model for the analysis of plates stiffened by parallel beams with deformable connection. Computers and Structures 86, 2166–2181.

Touzé, C., Thomas, O., Chaigne, A., 2002. Asymmetric nonlinear forced vibrations of free-edge circular plates. Part 1. Theory. Journal of Sound and Vibration 258, 649–676.